Current Biology *16*, 47–55, January 10, 2006 ©2006 Elsevier Ltd All rights reserved DOI 10.1016/j.cub.2005.11.070

Article

The Conserved Kinases CDK-1, GSK-3, KIN-19, and MBK-2 Promote OMA-1 Destruction to Regulate the Oocyte-to-Embryo Transition in *C. elegans*

Masaki Shirayama,[1,5] Martha C. Soto,[3,5] Takao Ishidate,[1,5] Soyoung Kim,[1,5] Kuniaki Nakamura,[1] Yanxia Bei,[1] Sander van den Heuvel,[4] and Craig C. Mello[1,2,*]

[1] Program in Molecular Medicine
[2] Howard Hughes Medical Institute
University of Massachusetts Medical School
373 Plantation Street
Worcester, Massachusetts 01605
[3] Department of Pathology
UMDNJ-RWJMS
Piscataway, New Jersey 08854
[4] Developmental Biology
Kruytbuilding N305
Padualaan 8
Utrecht University
3584 CH Utrecht
The Netherlands

Summary

Background: At the onset of embryogenesis, key developmental regulators called determinants are activated asymmetrically to specify the body axes and tissue layers. In *C. elegans*, this process is regulated in part by a conserved family of CCCH-type zinc finger proteins that specify the fates of early embryonic cells. The asymmetric localization of these and other determinants is regulated in early embryos through motor-dependent physical translocation as well as selective proteolysis.

Results: We show here that the CCCH-type zinc finger protein OMA-1 serves as a nexus for signals that regulate the transition from oogenesis to embryogenesis. While OMA-1 promotes oocyte maturation during meiosis, destruction of OMA-1 is needed during the first cell division for the initiation of ZIF-1-dependent proteolysis of cell-fate determinants. Mutations in four conserved protein kinase genes—*mbk-2*/Dyrk, *kin-19*/CK1α, *gsk-3*, and *cdk-1*/CDC2—cause stabilization of OMA-1 protein, and their phenotypes are partially suppressed by an *oma-1* loss-of-function mutation. OMA-1 proteolysis also depends on Cyclin B3 and on a ZIF-1-independent CUL-2-based E3 ubiquitin ligase complex, as well as the CUL-2-interacting protein ZYG-11 and the Skp1-related proteins SKR-1 and SKR-2.

Conclusions: Our findings suggest that a CDK1/Cyclin B3-dependent activity links OMA-1 proteolysis to completion of the first cell cycle and support a model in which OMA-1 functions to prevent the premature activation of cell-fate determinants until after they are asymmetrically partitioned during the first mitosis.

*Correspondence: craig.mello@umassmed.edu
[5] These authors contributed equally to this work.

Introduction

In many organisms, fertilization triggers a remarkable cascade of events, including cytoskeletal reorganization and the subsequent asymmetric localization of factors that regulate gene expression and cell fate [1]. In *C. elegans,* the initial anterior-posterior polarity of the embryo is established after fertilization and completion of female meiosis. Possible links between oocyte meiotic maturation and initial establishment of cell polarity have been reported previously. For example, prior to fertilization, sperm-derived signals trigger the completion of the meiosis I to II transition and promote ovulation [2–4], and after fertilization, interactions between the sperm-derived astral microtubules and the cortex of the embryo define the posterior pole. This initial polarity cue, in turn, triggers the actin/myosin-based partitioning of both cytoplasmic and cortical factors [5].

Among the developmentally important factors localized during this process are the transcriptional regulator SKN-1 and several members of the Cys3-His zinc finger protein family, including PIE-1 and MEX-5 [6–8].

The PIE-1 family member OMA-1 (also called MOE-1) and its close homolog OMA-2 are required for oocyte maturation [9, 10]. In the distal gonad, OMA protein levels are low due to GLD-1-dependent translational inhibition [11]. OMA protein levels begin to increase at the pachytene stage of meiosis I, reach a maximum level in the maturing oocyte, and quickly fall to much lower levels during the first mitosis [9, 10]. A gain-of-function *oma-1* mutation that stabilizes the OMA-1 protein results in mislocalization of PIE-1 and MEX-5 and induces an excess-endoderm phenotype that correlates with ectopic expression of the proendoderm transcription factor, SKN-1 [12]. OMA-1 destruction depends on the Dyrk-kinase homolog MBK-2, which also downregulates the Katanin homolog MEI-1 at the end of meiosis [13–15]. However, unlike MEI-1 protein, OMA-1 begins to disappear only after the fertilized egg enters the first mitosis. How the destruction of OMA-1 is timed to coincide with the first mitosis is not yet known.

The PIE-1 and MEX-5 proteins are present at high levels throughout the oocyte and fertilized egg, but they become localized asymmetrically to opposite ends of the embryo prior to the first mitosis. The MEX-5 protein is localized to the anterior half of the fertilized egg via a mechanism that depends on the PAR proteins [7]. MEX-5, in turn, promotes the posterior localization of PIE-1, and does so in part through the activation of the ZIF-1-dependent CUL-2-mediated proteolysis of PIE-1 in the anterior region of the embryo [16].

Here we describe several new mutants with phenotypes very similar to that of the previously described *oma-1* gain-of-function mutant. These mutations include two new alleles of *oma-1,* as well as two special alleles of the major cell-cycle kinase *cdk-1*, one allele of the 13 kDa CDK-1 binding partner, *cks-1,* and one allele of the Dyrk-kinase homolog, *mbk-2*. We show that all of

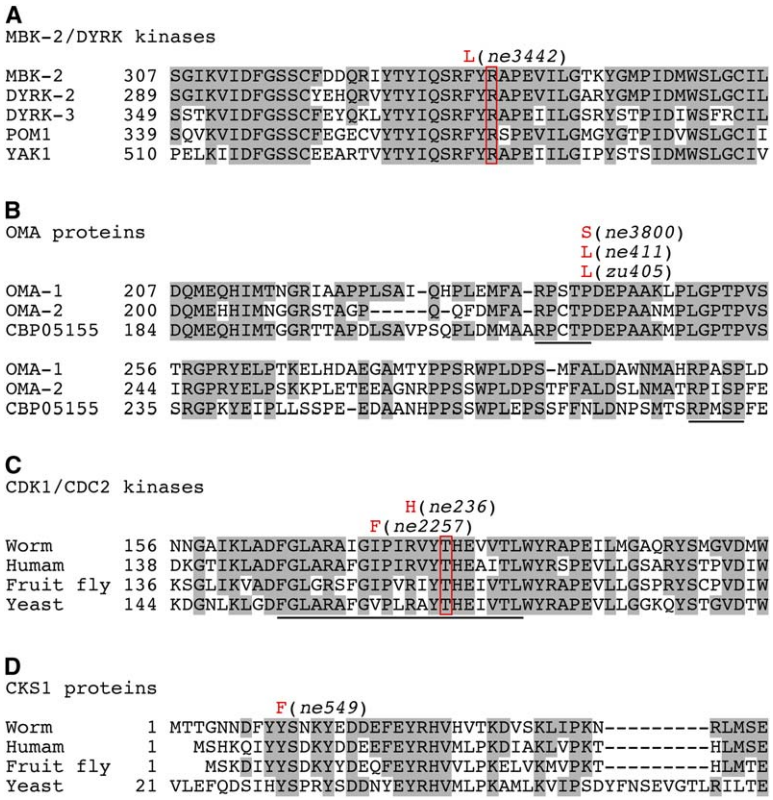

Figure 1. Identification of Extra-Gut Mutants

Partial amino acid sequence alignments for the MBK-2 protein and other Dyrk-family kinases including human Dyrk2 and 3, fission yeast Pom1, and budding yeast Yak1 (A), for the OMA-1 protein and its *C. elegans* and *C. briggsae* homologs (OMA-2 and CBP05155, respectively) (B), for the CDK-1 protein and its human, fruit fly, and budding yeast homologs (C), and for the CKS-1 protein and its human, fruit fly, and budding yeast homologs (D). The amino acid substitutions found in temperature-sensitive or maternal-effect lethal alleles of each protein are indicated in red above the corresponding residue in each alignment. In (A), an arginine residue that is required in proline-directed kinases for P+1 specificity is boxed in red. Potential MBK-2 phosphorylation sites in OMA-1 and its homologs are underlined in (B). In (C), a threonine residue that is phosphorylated by CAK kinase is boxed in red. The T loop/activation domain is underlined.

these mutants exhibit stabilization of OMA-1 and that all are suppressed in part by downregulating OMA-1 expression. OMA-1 destruction also requires Cyclin B3, the GSK-3 and KIN-19/CK1α kinases, a ZIF-1-independent CUL-2-based E3 ubiquitin ligase complex, the CUL-2-interacting protein ZYG-11, and the Skp1-related proteins SKR-1 and SKR-2. Our findings support a model in which OMA-1 functions to prevent the premature activation of cell-fate determinants and provide insights into regulatory mechanisms that link the asymmetric activation of determinants to the completion of the first cell cycle.

Results and Discussion

Isolation of Extra-Gut Mutants

In very large-scale screens for conditional and maternal-effect embryonic-lethal mutants, we identified several mutants with excess endoderm and a suite of other defects in cell polarity and cell-fate specification that were very similar to the phenotype caused by depletion of the conserved protein kinase GSK-3 [17] (see Figure S1 in the Supplemental Data available with this article online). We later found that these mutants were also similar phenotypically to a gain-of-function (*gf*) allele of the oocyte maturation factor *oma-1* [12]. For example, we found that all of these mutants exhibit mislocalization of cell-fate determinants such as PIE-1 and SKN-1 (Figure S2 and data not shown).

Our genetic and molecular studies revealed that these new mutants include one allele of the Dyrk family kinase homolog *mbk-2*(*ne3442*), two new gain-of-function alleles of *oma-1*(*ne411gf* and *ne3800gf*), two alleles of the cyclin-dependent protein kinase *cdk-1*(*ne236* and *ne2257*), and one allele of a highly conserved 13 kDa CDK-1-interacting protein, *cks-1*(*ne549*) (Figure 1).

Degradation of OMA-1 Depends on the MBK-2, CDK-1, and GSK-3 Kinases

All three gain-of-function *oma-1* mutants cause stabilization of the OMA-1 protein ([12] data not shown), and one of the genes identified in our screen, *mbk-2,* was recently linked to regulation of OMA-1 destruction [13]. We therefore asked whether the other newly identified mutant strains might also exhibit OMA-1 stabilization. In wild-type animals, OMA-1 and its homolog OMA-2 accumulate during oogenesis and remain high until the 1-cell stage, but rapidly decline during the first and second mitosis [9, 10] (Figure 2 and Figure S3). We examined the timing of OMA-1 degradation by monitoring the expression of an OMA-1::GFP protein. We found that OMA-1 protein levels remain high in *gsk-3*, *cdk-1*, *cks-1*, and *mbk-2* mutant embryos (Figure 2, Figure S3, and data not shown). Furthermore, consistent with the idea that the cell-fate defects in these mutants result from OMA-1 (and to some extent OMA-2) stabilization, we found that each mutant was suppressed by loss-of-function *oma-1* (or *oma-2*) mutations (Table 1, and data not shown). In the case of the *cdk-1(ne2257)* and *gsk-3(nr2047)* mutants, substantial suppression was observed in *oma-1* (*te33)* mutants (Table 1). The *mbk-2*(*ne3442*) mutant was only weakly suppressed by *oma-1*(*te33*) (Table 1).

These results suggest that the *mbk-2(ne3442)* mutation also affects additional developmental functions of MBK-2 [13]. Likewise, the incomplete suppression observed in *cdk-1* and *gsk-3* backgrounds by *oma-1(te33)* loss of function could reflect the existence of defects in developmental mechanisms unrelated to

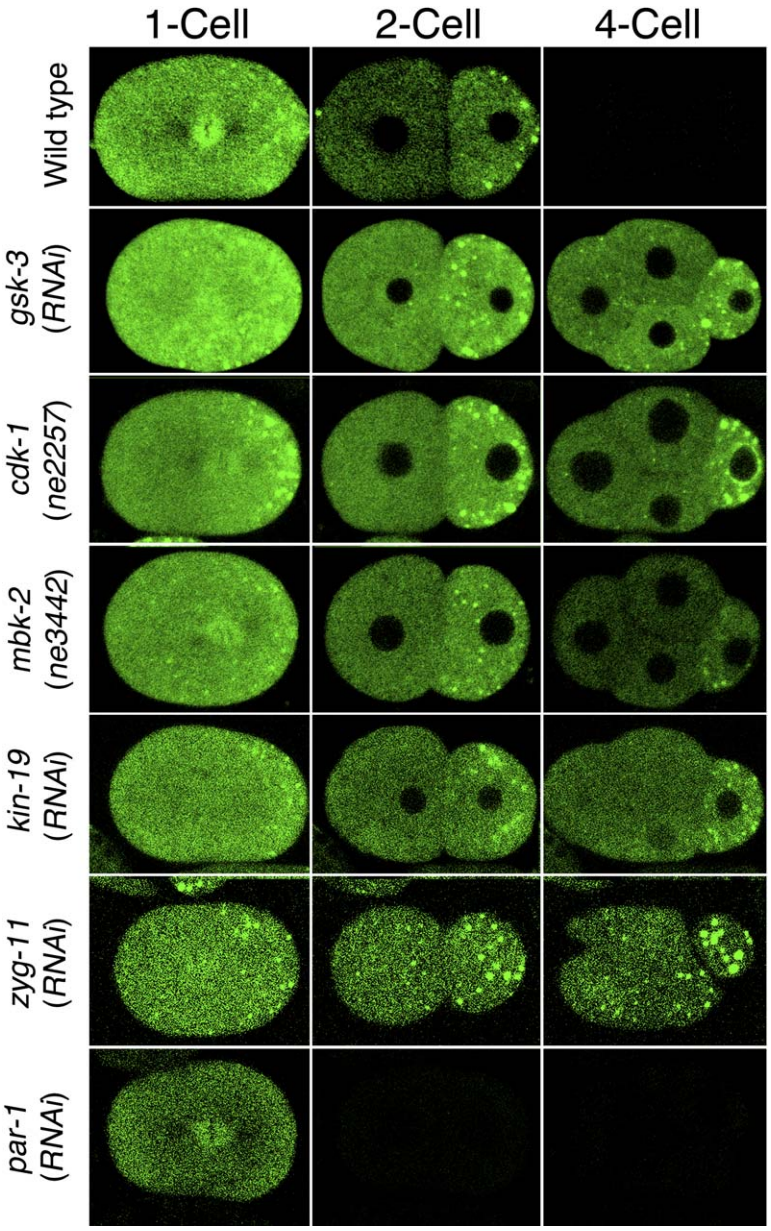

Figure 2. *mbk-3, gsk-3*, and *cdk-1* Are Defective in OMA-1 Proteolysis

Fluorescence micrographs showing OMA-1::GFP in wild-type and mutant embryos at three time points (as indicated). The row labels in this figure are correct and have been slightly modified from the version of this paper published online December 8, 2005.

Table 1. Phenotypic and Rescue Analysis of Extra-Gut Mutants

Genotype	C-Derived Gut[a]	EMS Division (L/R)
Wild-type	0% (0/6)	0% (0/8)
oma-1(*zu405*)[b]	80%	50%
gsk-3(*nr2047*)	43% (6/14)	59% (10/17)
gsk-3(*nr2047*); *oma-1*(*te33*)	14% (1/7)	5.9% (1/17)
cdk-1(*ne2257*)	36% (4/11)	95% (19/20)
cdk-1(*ne2257*); *oma-1*(*te33*)	10% (1/10)	0% (0/10)
mbk-2(*ne3442*)	100% (12/12)	92% (11/12)
mbk-2(*ne3442*) *oma-1*(*te33*)	78% (18/23)	41% (7/17)

[a] C-derived gut specification was followed in laser-operated embryos.
[b] Phenotype of *oma-1* (*zu405*) was previously scored by Lin [12].

OMA-protein stabilization. However, given that partial suppression was also observed in *oma-2* loss-of-function mutants, it is likely that the failure to achieve full suppression reflects, at least in part, the persistence of the OMA-2 protein in these double mutant backgrounds. Unfortunately, it is not possible to construct triple mutant embryos lacking both OMA proteins due to the requirement for at least one intact *oma* gene for oocyte maturation.

GSK3 and KIN-19 Influence Wnt Signaling Indirectly through OMA-1

Endoderm specification is regulated by both the Wnt [18, 19] and Src [20] pathways in *C. elegans*. A previous

study has shown that the Wnt-responsive Tcf/Lef-related protein POP-1 is misregulated in *oma-1*(*zu405gf*) mutants [12], and we found that SRC-1-dependent phosphotyrosine staining at the junction between signaling cells is reduced in *oma-1*(*ne411gf*) mutants (data not shown). These findings suggest that stabilized OMA-1 interferes with both the Wnt- and Src-signaling pathways, perhaps by perturbing the localization of SKN-1, PIE-1, and other upstream maternal determinants that specify the fates of the signaling and responding cells.

Previous genetic studies have suggested that GSK-3 and a Casein kinase 1α (CK1α) homolog, KIN-19, have direct functions in the Wnt/wingless pathway for endoderm specification and spindle orientation [17, 21, 22]. We found that *RNAi* targeting *kin-19* also causes OMA-1 stabilization (Figure 2 and Figure S3). The finding that both kinases are required for OMA-1 proteolysis and that the cell fate and spindle-orientation defects of *gsk-3* mutants are suppressed by lowering OMA-1 levels suggests that these kinases may indirectly regulate P2/EMS signaling by lowering OMA protein levels in early embryos.

OMA-1 Ubiquitination Machinery

In a previous genetic screen, we identified one additional mutant allele, *zu136,* which exhibits an extra-endoderm phenotype similar to that of *oma-1*(*gf*). Genetic mapping and complementation analysis revealed that *zu136* is allelic to *zyg-11*. Although the molecular function of ZYG-11 is not yet determined, it has been reported that ZYG-11 acts with a CUL-2-based E3 ubiquitin-ligase to control progress through meiosis II [23, 24]. Degradation of OMA-1 was previously reported to depend on CUL-2 [16]. We therefore examined the role of ZYG-11 and found that OMA-1 degradation is disrupted in *zyg-11*(*RNAi*) embryos (Figure 2 and Figure S3). Similar results were obtained in *zyg-11*(*zu136*) mutants (data not shown). Thus, the destruction of OMA-1, like the destruction of PIE-1 and other maternal determinants, depends on a CUL-2/E3 complex [16]. However, OMA-1 differs from PIE-1 in that its destruction is not dependent on the SOCS protein ZIF-1 [16]. This difference in the adaptor proteins required for destruction of OMA-1 versus other zinc finger family members may help explain how OMA-1 destruction precedes and appears to regulate the destruction of PIE-1 (see below).

CUL-2 is a core component of the ECS (Elongin C-Cul2-SOCS box) E3 ubiquitin ligase complex. However, we found that *RNAi* targeting *elc-1* (elongin C), *elb-1* (elongin B), or both caused, at most, a modest increase in OMA-1 levels (data not shown). Instead, we found that destruction of OMA-1 is largely dependent on the Skp1 homologs SKR-1 and SKR-2 (data not shown). Since it has been reported that both SKR-1 and SKR-2 interact with CUL-1 as an SCF (Skp1-Cul1-F-box) complex, but not with CUL-2 [25, 26], it is unclear at present whether SKR-1 and SKR-2 work directly with CUL-2 in OMA-1 destruction.

The *zyg-11, skr-1/skr-2*, and *cul-2* mutant embryos have pleiotropic effects on polarity and may thus indirectly affect OMA-1 degradation. In order to test the possibility that the timing of OMA-1 proteolysis is influenced by cell-polarity factors, we examined OMA-1 localization in *par-1*(*RNAi*) embryos [27]. We found that OMA-1 degradation is still coupled to the cell cycle and occurs as in wild-type embryos, at the onset of the first mitosis (Figure 2). This result suggests that initiation of OMA-1 degradation is not regulated by *par-1*-dependent anterior-posterior cell polarity. However, whereas OMA-1 disappears more slowly from the posterior blastomere P1 in wild-type embryos, we observed that OMA-1 instead disappears almost simultaneously from both 2-cell stage blastomeres in *par-1* mutants (Figure 2).

mbk-2(ne3442), cdk-1(ne236 and *ne2257),* and *cks-1(ne549)* Are Nonnull Alleles

The newly identified alleles of *cdk-1*, *cks-1*, and *mbk-2* are nonnull alleles. Null alleles of each of these mutants exhibit additional phenotypes, including sterility and cell-division defects (in the case of *cdk-1* and *cks-1* mutants) and polarity and spindle-positioning defects (in the case of *mbk-2* null mutants) [13–15]. The *mbk-2* (*ne3442)* allele is a temperature-sensitive mutation that alters a conserved amino acid located just two amino acids away from an arginine residue required for substrate recognition in proline-directed kinases [28] (Figure 1A). The proximity of the *ne3442* lesion to this conserved residue could alter substrate recognition by the mutant protein and may thus explain why this allele is strongly defective in OMA-1 destruction but exhibits no apparent defects in other MBK-2 functions required for microtubule stability and spindle positioning [13–15] (data not shown).

CDK-1 and its 13 kDa binding partner CKS-1 are essential cell-cycle regulators that are highly conserved from yeast to humans. Depletion of maternal *cdk-1* or *cks-1* by *RNAi* causes a 1-cell meiotic arrest [29, 30]. In contrast, *cdk-1*(*ne236)*, *cdk-1(ne2257*), and *cks-1*(*ne549*) homozygotes have no obvious larval phenotypes and produce mutant embryos with normal cell divisions and well-differentiated cells and tissues (Figure S1, data not shown). Both CDK-1 mutations alter residues within the T loop (or activation loop) of CDK-1 (Figure 1C), a region implicated in cyclin binding [31]. The CKS-1 lesion is predicted to disrupt a single intramolecular hydrogen bond based on the crystal structure of CKS-1 [32] (Figure 1D).

CDK1/CDC2 kinases are regulated in part through their interactions with cyclins. We therefore used *RNAi* to search for cyclins required for OMA-1 destruction. The *C. elegans* genome contains a single cyclin A gene (*cya-1*), three cyclin B genes (*cyb-1*, *cyb-2.1*, and *cyb-2.2*), and a single cyclin B3 gene (*cyb-3*) [33]. Despite the cell-cycle delay associated with cyclin *RNAi* [34], we found that OMA-1 protein is degraded with normal timing, as cells first enter mitosis, in cyclin A- or cyclin B-depleted embryos (Figure 3). In contrast, we found that OMA-1 protein is dramatically stabilized in embryos depleted for cyclin B3 (Figure 3).

We next examined the effects of the mutations in CDK-1 and CKS-1 proteins on their activities and interactions with each other and with Cyclin B and Cyclin B3. We found that the CDK-1 protein encoded by the *ne2257* mutant allele, CDK-1(I173F), binds to CKS-1, CYB-1, and CYB-3 as efficiently as does wild-type CDK-1 (Figures 4A, 4B, and 4E) and that both cyclin complexes recovered from *cdk-1*(*ne2257*) mutant extracts exhibit near wild-type activity toward histone H1 (Figures 4A and 4B). In contrast, we found that the CKS-1 protein

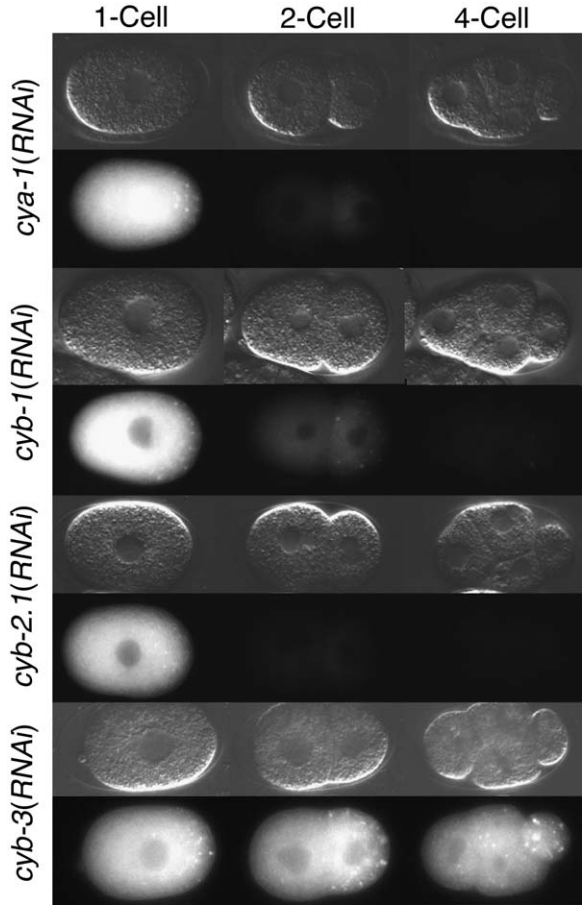

Figure 3. Cyclin B3 Is Specifically Required for OMA-1 Proteolysis

Nomarski and fluorescence micrographs (upper and lower rows, respectively) showing OMA-1::GFP localization in various cyclin-depleted embryos (as indicated).

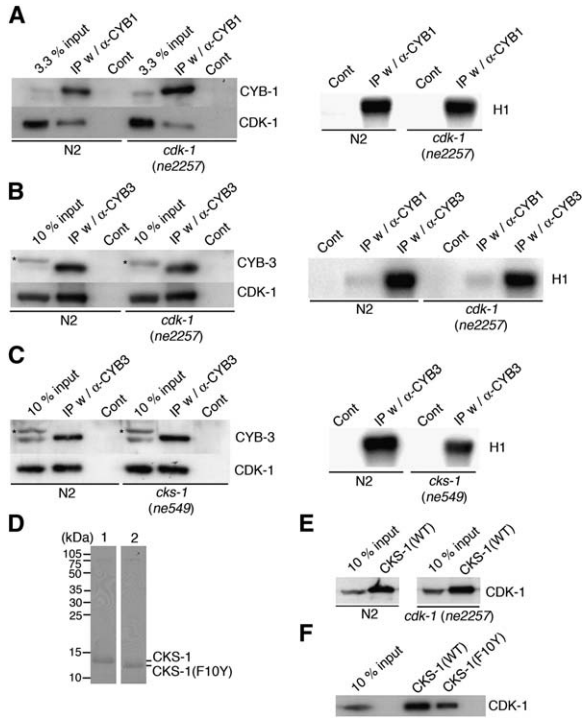

Figure 4. Characterization of CDK-1/CKS-1/Cyclin Complexes

(A–C) Characterization of CDK-1/cyclin complexes by coimmunoprecipitation (left) and by histone-H1 kinase assay (right). Immunoprecipitations were conducted on wild-type and mutant extracts with either no antibodies (lanes labeled "Cont") or antibodies specific for CYB-1 ([A], left) or CYB-3 ([B] and [C], left) and were visualized via Western blotting with Cyclin and CDK-1-specific antisera (as indicated). CYB-3 antisera recognize a prominent background band (*) that is not depleted in *cyb-3* (*RNAi*) mutant extracts (data not shown). Complexes recovered in (A)–(C) (left) were incubated with Histone H1 and radioactive ATP, and phosphorylation of histone-H1 was measured by autoradiography ([A]–[C], right). For comparison, CYB-1 and CYB-3 kinase activities were detected in the same blot ([B], right), while a longer exposure of the CYB-1 blot is also provided ([A], right). The difference in the amount of active CDK-1 recovered by the CYB-1 and CBY-3 sera could merely reflect differences in the nature of the antibodies and may not reflect the actual relative levels or activities of these complexes in vivo. For example, the CYB-1 antibodies may interfere with or reduce CDK-1 binding or activity.

(D) Bacterially expressed wild-type CKS-1 and mutant CKS-1 (F10Y, encoded by *ne549*) were visualized by Coomassie staining.

(E and F) Characterization of CDK-1/CKS-1 complexes by pull-down assay with CKS-1-associated beads in *cdk-1* (*ne2257*) mutant (E) and CKS-1 or CKS-1 (F10Y)-associated beads in wild-type extract (F).

encoded by *ne549*, CKS-1(Y10F), exhibits reduced binding to wild-type CDK-1 (Figure 4F) and, although the binding of CDK-1 to the cyclins was not altered detectably, we found that CDK-1/CYB-3 activity toward histone H1 is reduced to 60% of wild-type in *cks-1*(*ne549*) mutants (Figure 4C). Taken together, these findings suggest that, consistent with the lack of visible defects in the cell cycle, these alleles exhibit, at most, weak effects on the histone-H1 kinase activity of the CYB-1 and CYB-3 complexes.

MBK-2 Phosphorylates OMA-1

Since OMA-1 degradation is impaired in *mbk-2*, *gsk-3, kin-19*, and *cdk-1* mutants, we hypothesized that some or all of these protein kinases may directly phosphorylate OMA-1. Scanning of the OMA-1 sequence revealed two potential MBK-2 phosphorylation sites (T239 and S302) [28] that are conserved among *C. elegans* and *C. briggsae* OMA proteins (Figures 1B and 5A). Interestingly, T239 is located next to proline 240, which is mutated in both the original and our newly identified OMA-1 gain-of-function alleles [12] (Figure 1B). We found that MBK-2 efficiently phosphorylates both potential MBK-2 sites in these OMA-1 fragments (Figure 5B). Furthermore, when both potential MBK-2 sites were mutated (S238A; T239A or S302A), the phosphorylation of the corresponding fragments was abolished. Importantly, the proline to leucine change (P240L) found in the *oma-1* gain-of-function mutants (*zu405* and *ne411*) also prevented phosphorylation at T239 (Figure 5B). Taken together, these results suggest that MBK-2 can phosphorylate OMA-1 on T239 and S302 in vitro and that phosphorylation of T239 (at least) is important for the destruction of OMA-1 protein in vivo.

We did not detect any CDK-1-dependent phosphorylation of OMA-1 (data not shown), suggesting that CDK-1 may not directly regulate OMA-1. In contrast, we found

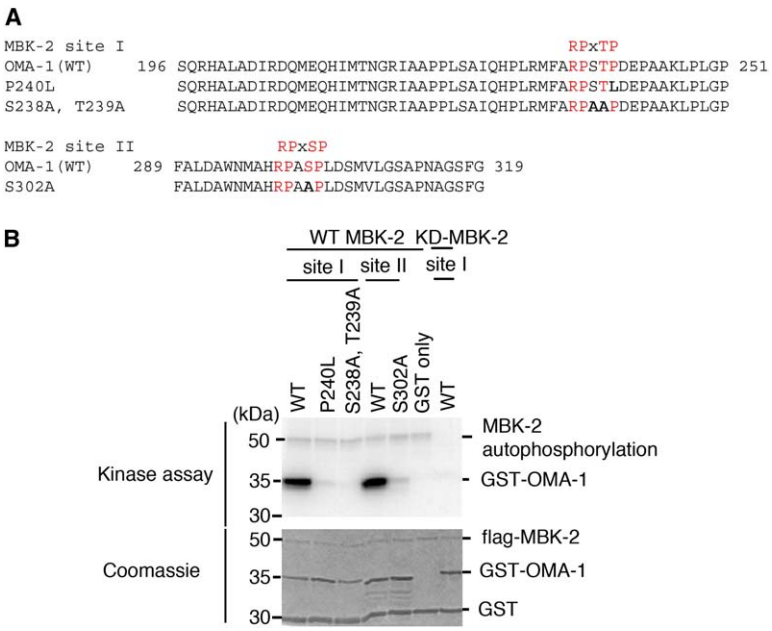

Figure 5. Analysis of OMA-1 Phosphorylation by MBK-2

(A) Alignments of wild-type (wt) and mutant OMA-1 protein fragments. Amino acids altered in the mutant isoforms are shown in bold type. Putative MBK-2 target sites are indicated in red.

(B) Kinase assays performed by incubating the indicated wt and mutant OMA-1 substrates with wt and kinase dead (KD) MBK-2. Kinase activity is measured by autoradiography to detect radioactive ^{32}P incorporation into the OMA-1 substrates (top), while relative amount of protein used as substrate in each lane indicated by Coomassie staining (bottom).

that both human CK1 (a very close homolog of KIN-19) and *C. elegans* GSK-3 exhibit weak activity toward full-length OMA-1 protein and that this activity is enhanced after pretreatment of OMA-1 with MBK-2 (Figure S4). These findings suggest that KIN-19 and GSK-3 may directly phosphorylate OMA-1 in an MBK-2-dependent manner.

OMA-1 Inhibits ZIF-1-Dependent Proteolysis of PIE-1

Stabilization of OMA-1 in early embryos is correlated with the persistent expression of several other key developmental regulators [12] (Figure S2). This raises the possibility that the OMA proteins may normally function in early embryos to prevent the premature destruction of these developmental regulators. The soma-specific degradation of PIE-1 and of other CCCH-type zinc finger proteins such as MEX-1 and POS-1 depends on a CUL-2/E3 complex and its substrate-specific component ZIF-1 [16]. In order to ask if stabilized OMA-1 interferes with ZIF-1-dependent proteolysis, we employed an assay system described by DeRenzo et al. [16] that utilizes a *par-1* mutant background and a GFP construct fused to the first zinc-finger domain (ZF1) of PIE-1 (GFP::ZF1) to follow ZIF-1-dependent destruction. In *par-1* mutants, GFP::ZF1 protein is expressed uniformly in all blastomeres until the 2-cell stage but is degraded rapidly when the embryo divides from two to four cells. This degradation is dependent on ZIF-1. We found that in *gsk-3*(*RNAi*), *cdk-1*(*ne2257*), and *oma-1*(*ne411gf*) mutants, the GFP::ZF1 signal remains high from the 4- to 8-cell stage (Figure 6A), suggesting that stabilized OMA-1 interferes with ZIF-1-dependent proteolysis. It was previously shown that MEX-5 activates ZIF-1-dependent proteolysis [16]. Since both MEX-5 and OMA-1 are CCCH-type zinc finger proteins similar to the RNA binding protein TIS11 [35], it is possible that they exert their effects by regulating the translation of the *zif-1* mRNA.

OMA-1 Destruction and Its Implications

Our findings support a model in which OMA-1 functions to prevent the premature destruction of maternal factors until after the first asymmetric division of the embryo (Figure 6B). In oocytes and newly fertilized embryos, PIE-1 and MEX-5 coexist within the cytoplasm. However, after fertilization, these proteins rapidly become localized to opposite regions of the 1-cell embryo in a manner that depends on the PAR proteins and the actin cytoskeleton [36]. During this process, the majority of the PIE-1 protein becomes localized to the posterior of the 1-cell embryo. Following the first mitosis, MEX-5-dependent activity, now enriched in the anterior blastomere, promotes the ZIF-1-dependent proteolysis of any residual PIE-1 protein present in the anterior of the embryo. Conceivably, OMA-1 inhibits ZIF-1-dependent proteolysis to permit PIE-1 and MEX-5 to coexist in the embryo prior to the first asymmetric division. Destruction of OMA-1 at the end of the first mitosis might then be an important trigger that helps to drive the asymmetric expression of PIE-1.

According to this model, when MBK-2 phosphorylates and promotes destruction of the microtubule-severing Katanin homolog MEI-1 during meiosis (Stitzel et al., this issue of *Current Biology* [37]), MBK-2 may simultaneously phosphorylate OMA-1 (this work, [37, 38]). However, unlike MEI-1, OMA-1 is not degraded until after the first mitosis. Instead, further regulatory events involving KIN-19, GSK-3, and CDK-1 are required for OMA-1 destruction. These events may include direct phosphorylations that depend on a conformational change in OMA-1 or changes in the localization of the regulators. Consistent with this idea, it has been recently shown that OMA-1 is directly phosphorylated by GSK-3 and that this phosphorylation is important for OMA-1 destruction [38]. Regulation by CDK-1 provides an important link between OMA-1 proteolysis and completion of the first cell cycle and may thus guarantee that ZIF-1/CUL-2/E3-dependent proteolysis commences only

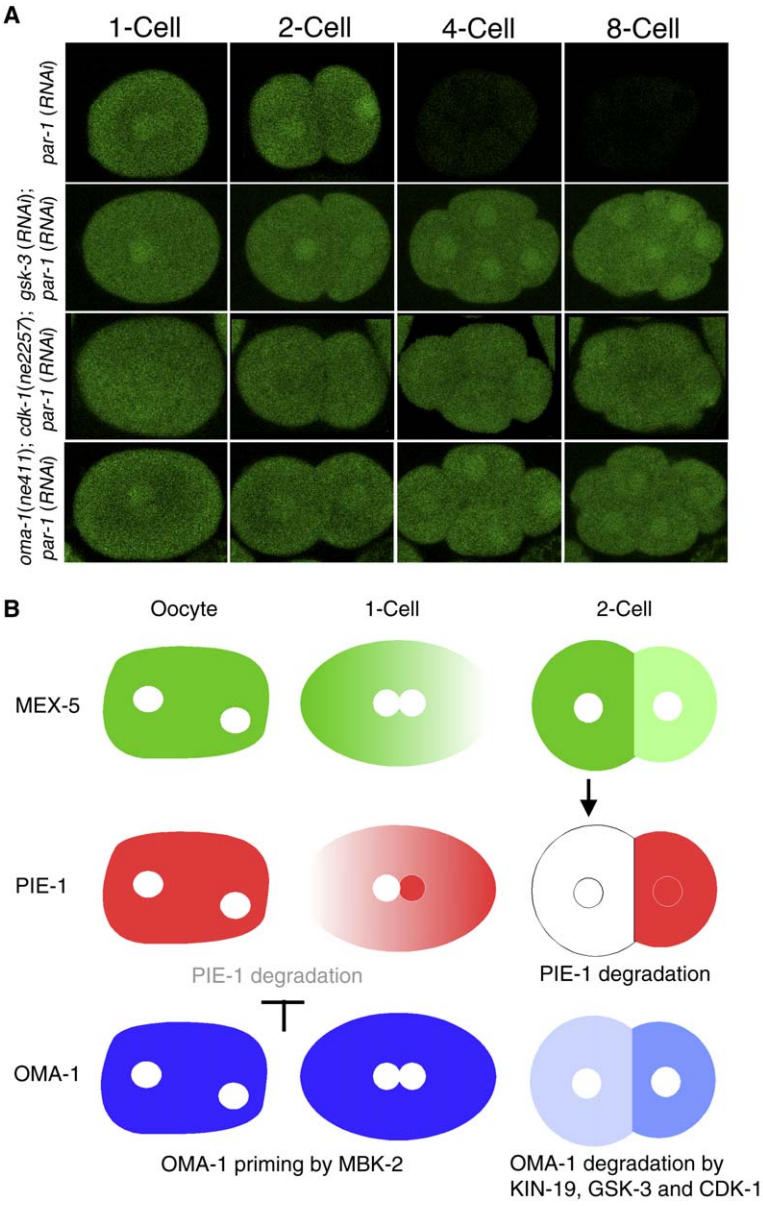

Figure 6. OMA-1 Degradation Regulates ZIF-1-Dependent Proteolysis

(A) Fluorescence micrographs showing GFP::ZF1 (PIE-1) localization in *par-1*(*RNAi*) single mutant embryos and in *par-1*(*RNAi*); *gsk-3*(*RNAi*), *par-1*(*RNAi*); *cdk-1*(*ne2257*), and *par-1*(*RNAi*); *oma-1*(*ne411*, gain-of-function) double mutant embryos. Sequential images were taken from individual embryos at the indicated cell stages. At least three embryos were followed from the 1-cell stage for each mutant and similar results were obtained.

(B) Model for how OMA-1 degradation may determine the timing of ZIF-1-dependent proteolysis. Schematic diagrams showing the localization of MEX-5 (green), PIE-1 (red), and OMA-1 (blue). High levels of OMA-1, indicated by the bright blue color of the oocyte and 1-cell stage embryos, prevents ZIF-1-dependent proteolysis of PIE-1 (indicated by the genetic bar in bold between the red and blue diagrams). Although the initial phosphorylation of OMA-1 by MBK-2 may occur during meiosis, subsequent phosphorylations by KIN-19 and GSK-3 may be delayed or are insufficient to induce OMA-1 destruction, until after CDK-1/CYB-3 is activated at the first mitosis (indicated by the fading blue color). The degradation of OMA-1 at this time permits the activation of MEX-5/ZIF-1-dependent proteolysis of PIE-1 in the anterior daughter cell.

Panel (B) in the figure shown here has been corrected from the one originally published online, where the gradient distribution of MEX-5 in the 1-cell stage was not indicated.

after MEX-5 and PIE-1 are physically partitioned by cytokinesis.

There are precedents for CDK1/CDC2 as a regulator of cell polarity. For example, a mutation that reduces *Drosophila* CDK1 activity results in a loss of polarity in neuroblasts, supporting a model in which different thresholds of CDK1 kinase activity are required for the cell-cycle and polarity functions of CDK1 [39]. In contrast, our *cdk-1*(*ne2257*) mutants exhibit wild-type kinase activity toward histone H1 and may thus perturb the recognition of only a subset of CDK-1 substrates, or may perturb kinase-independent activities of the CKS-1 and CDK-1 proteins [40]. How cell-fate specification and polarity-signaling mechanisms are linked to the cell cycle remains almost entirely unknown at present. The special alleles of *cdk-1* and *cks-1* described here provide rare and important clues to these fundamental mechanisms.

Experimental Procedures

Genetics

All strains were handled and cultured as described by Bei et al. [20]. The temperature-sensitive embryonic lethal screening was performed as described in Pang et al. [15].

RNA Interference

RNA interference (*RNAi*) was performed as described in Bei et al. [20] by feeding or injecting double-stranded (ds) RNA at concentration of 1 mg/ml for single dsRNA and 1 mg/ml each for double dsRNAs injection. Embryos collected 24 hr after injection were scored for phenotypes at the appropriate temperature.

Plasmid Construction

A full-length MBK-2 cDNA was cloned in the *Bam*HI/*Xho*I sites of the pCCM803 vector downstream of the CMV promoter and in-frame with three copies of the flag epitope tag. This cDNA includes an additional exon at the 3′ end (exon 7) that is not annotated in Wormbase [15]. The MBK-2 kinase dead (KD) mutation (K196R) in the kinase catalytic domain of MBK-2 was created by in vitro mutagenesis. A

full-length GSK-3 cDNA was cloned in the *Hin*dIII/*Xba*I sites of pCCM802 downstream of the CMV promoter and in-frame with three copies of the myc epitope tag. To express GST-OMA-1 fusion proteins, we amplified various coding regions of OMA-1 by PCR and inserted the PCR fragments into *Eco*RI and *Sal*I sites of pET42a. The following plasmids were used to express GST-OMA-1 constructs in *E. coli*, BL21(*de3*), as follows: B1096 (full-length OMA-1); B1088 (COOH-terminal aa 215–407); B1169 (OMA-1 aa 215–407, T239A); B1176 (OMA-1 aa 215–407, T239A; S302A); B1082S1 (OMA-1 aa 196–251); B1082S2 (OMA-1 aa 196–251, P240L); B1082S3 (OMA-1 aa 196–251, S238A; T239A); B1084S7 (OMA-1 aa 289–319); and B1084S8 (OMA-1 aa 289–319, S302A).

Cell Culture and Transfection

COS cells were maintained in Dulbecco's Modified Eagle Medium (GIBCO) supplemented with 10% fetal bovine serum (HyClone). For transfection experiments, cells grown on 10 cm dishes were transfected with 2 μg of plasmid DNA using Effectene reagent (QIAGEN) according to manufacturer's instructions.

Immunoprecipitation and Kinase Assays

COS cells were transfected with plasmids expressing flag-tagged MBK-2 or myc-tagged GSK-3. After 24 hr of incubation, the cells were lysed in lysis buffer (50 mM Tris HCl [pH 7.4], 1% NP-40, 150 mM NaCl, 5 mM DTT, 50 mM β-glycerophosphate, 1 mM sodium vanadate [ortho], 0.05 mM NaF, 0.1 mM PMSF supplemented with Complete Mini protease inhibitor cocktail tablet [Roche]), and insoluble material was removed by centrifugation. Flag-MBK-2 and myc-GSK-3 were then immunoprecipitated from the lysates by anti-flag or anti-myc antibodies conjugated to agarose beads (Sigma). Beads were washed three times with lysis buffer and twice with kinase buffer, and then aliquoted for kinase assays.

For CK1 kinase assays, N-terminally GST-tagged rat CK1δ purchased from Upstate (14-427) was used. Kinase assays were done in kinase buffer (50 mM HEPES [pH 7.4], 10 mM $MgCl_2$, 10 mM DTT, 0.5 mM NaF, 0.1 mM Sodium vanadate [ortho], 100 μM ATP, 5 μg/ml leupeptin, and [γ-^{32}P]ATP [6000 Ci/mmol; Amersham]) for 15 min at 25ºC. For MBK-2/CK1 or MBK-2/GSK-3 sequential kinase assays, substrate was first incubated with MBK-2 immobilized on agarose beads in the presence of 100 μM of nonradiolabeled ATP, and then transferred to a fresh tube to which CK1 or GSK-3 and [γ-^{32}P]ATP were added.

For CDK-1 immunoprecipitation and kinase assay, wild-type(N2), *cdk-1*(*ne2257*), and *cks-1*(*ne549*) mutants were grown at 15ºC and shifted to 25ºC at L4 stage. Eggs were collected from each strain at 25ºC and lysed in ice-cold CDK-1 buffer (50 mM Tris HCl [pH 7.4], 150 mM NaCl, 15 mM $MgCl_2$, 1% NP-40, 60 mM β-glycerophosphate, 1 mM DTT, 0.1 mM Sodium vanadate [ortho], 0.1 mM PMSF, supplemented with Complete Mini protease inhibitor cocktail tablet [Roche]). After insoluble material was removed by centrifugation twice, CYB-1 or CYB-3 proteins were immunoprecipitated from the lysates by 1 hr incubation with anti-CYB-1 (1/5 dilution) or anti-CYB-3 (1/5 dilution) antibodies followed by another 1 hr incubation with Protein G beads (Roche) at 4ºC. Beads were washed three times with CDK-1 buffer and then boiled with SDS-PAGE sample buffer for immunoblotting. For kinase assays, beads were washed once more with 25 mM MOPS (pH 7.2), aliquoted, suspended into 6 μl of CDK-1 assay buffer (25 mM MOPS [pH 7.2], 60 mM β-glycerophosphate, 15 mM $MgCl_2$, 1 mM DTT, 1 mM PMSF, 0.1 mM Sodium vanadate [ortho]), and incubated at room temperature for 5 min. Prewarmed beads were added to 10 μl of cocktail containing 25 mM MOPS (pH 7.2), 2 mg/ml Histone H1 (Roche), and [γ-^{32}P]ATP (6000 Ci/mmol; Amersham) and incubated for 15 min at 25ºC. For CKS-1 pull-down assays, wild-type and mutant (F10Y encoded by *ne549*) CKS-1::HIS(3x) proteins were expressed in *E. coli*, purified via Ni column, and crosslinked to Sepharose 4B (Pharmacia Biotech) beads. Extracts from wild-type and *cdk-1*(*ne2257*) embryos grown at 25ºC were incubated with CKS-1 beads, and associated CDK-1 proteins were detected by immunoblotting.

Live Embryo Imaging and Antibody Staining

Embryos harboring various GFP constructs were mounted in water on glass slides covered with 2% agarose. DIC and GFP images were captured at every 20 s with a Leica confocal microscope. For GFP images, at least three embryos were followed from the 1-cell stage in each strain and similar results were obtained. SKN-1 staining was performed as described previously [8] and multiple embryos were scored.

Supplemental Data

Supplemental Data include three figures and five movies and can be found with this article online at http://www.current-biology.com/cgi/content/full/16/1/47/DC1/.

Acknowledgments

We are greatly indebted to Dr. Golden for the CDK-1 antibodies, Dr. Lin for the OMA-1::GFP transgenic worms and *oma-1*::*gfp* construct, Drs. Shimada, Kawahara, and Lin for OMA-1 and OMA-2 antibodies, and Dr. Seydoux for the GFP::PIE-1 and GFP::ZF1 transgenic worms. We are also grateful to Drs. J. Mello, Conte, Maekawa, and Kawahara for critical reading of this manuscript. We thank *C. elegans* Genetic Center for strains. This publication was made possible in part by grant HD036247 from the National Institutes of Health (NIH) and by postdoctoral grants from the America Cancer Society and the NIH to M.C.S. The contents of this article are solely the responsibility of the authors and do not necessarily represent the official views of the NIH.

Received: September 19, 2005
Revised: November 18, 2005
Accepted: November 23, 2005
Published online: December 8, 2005

References

1. Goldstein, B., and Freeman, G. (2005). Axis specification in animal development. Bioessays *19*, 105–116.
2. McCarter, J., Bartlett, B., Dang, T., and Schedl, T. (1999). On the control of oocyte meiotic maturation and ovulation in *Caenorhabiditis elegans*. Dev. Biol. *205*, 111–128.
3. Miller, M.A., Nguyen, V.Q., Lee, M.-H., Kosinski, M., Schedl, T., Caprioli, R.M., and Greenstein, D. (2001). A sperm cytoskeletal protein that signals oocyte meiotic maturation and ovulation. Science *291*, 2144–2147.
4. McNally, K.L., and McNally, F.J. (2005). Fertilization initiates the transition from anaphase I to metaphase II during female meiosis in *C. elegans*. Dev. Biol. *282*, 218–230.
5. Schnabel, R., and Priess, J.R. (1997). Specification of cell fates in the early embryo. In *C. elegans* II, D.L. Riddle, T. Blumenthal, B.J. Meyer, and J.R. Priess, eds. (Cold Spring Harbor, NY: Cold Spring Harbor Laboratory Press), pp. 361–382.
6. Mello, C.C., Schubert, C., Draper, B., Zhang, W., Lobel, R., and Priess, J.R. (1996). The PIE-1 protein and germline specification in *C. elegans* embryos. Nature *382*, 710–712.
7. Schubert, C.M., Lin, R., de Vries, C.J., Plasterk, R.H., and Priess, J.R. (2000). MEX-5 and MEX-6 function to establish soma/germline asymmetry in early *C. elegans* embryos. Mol. Cell *5*, 671–682.
8. Bowerman, B., Draper, B.W., Mello, C.C., and Priess, J.R. (1993). The maternal gene *skn-1* encodes a protein that is distributed unequally in early *C. elegans* embryos. Cell *74*, 443–452.
9. Detwiler, M.R., Reuben, M., Li, X., Rogers, E., and Lin, R. (2001). Two zinc finger proteins, OMA-1 and OMA-2, are redundantly required for oocyte maturation in *C. elegans*. Dev. Cell *1*, 187–199.
10. Shimada, M., Kawahara, H., and Doi, H. (2002). Novel family of CCCH-type zinc-finger proteins, *MOE-1, -2* and *-3*, participates in *C. elegans* oocyte maturation. Genes Cells *7*, 933–947.
11. Lee, M.-H., and Schedl, T. (2004). Translation repression by GLD-1 protects its mRNA targets from nonsense-mediated mRNA decay in *C. elegans*. Gene & Dev *18*, 1047–1059.
12. Lin, R. (2003). A gain-of-function mutation in *oma-1*, a *C. elegans* gene required for oocyte maturation, results in delayed degradation of maternal proteins and embryonic lethality. Dev. Biol. *258*, 226–239.
13. Pellettieri, J., Reinke, V., Kim, S.K., and Seydoux, G. (2003). Coordinate activation of maternal protein degradation during the egg-to-embryo transition in *C. elegans*. Dev. Cell *5*, 451–462.

14. Quintin, S., Mains, P.E., Zinke, A., and Hyman, A.A. (2003). The *mbk-2* kinase is required for inactivation of MEI-1/katanin in the one-cell *Caenorhabditis elegans* embryo. EMBO Rep. *4*, 1175–1181.
15. Pang, K.M., Ishidate, T., Nakamura, K., Shirayama, M., Trzepacz, C., Schubert, C.M., Priess, J.R., and Mello, C.C. (2004). The minibrain kinase homolog, *mbk-2*, is required for spindle positioning and asymmetric cell division in early *C. elegans* embryos. Dev. Biol. *265*, 127–139.
16. DeRenzo, C., Reese, K.J., and Seydoux, G. (2003). Exclusion of germ plasm proteins from somatic lineages by cullin-dependent degradation. Nature *424*, 685–689.
17. Schlesinger, A., Shelton, C.A., Maloof, J.N., Meneghini, M., and Bowerman, B. (1999). Wnt pathway components orient a mitotic spindle in the early *Caenorhabditis elegans* embryo without requiring gene transcription in the responding cell. Genes Dev. *13*, 2028–2038.
18. Rocheleau, C.E., Downs, W.D., Lin, R., Wittmann, C., Bei, Y., Cha, Y.H., Ali, M., Priess, J.R., and Mello, C.C. (1997). Wnt signaling and an APC-related gene specify endoderm in early *C. elegans* embryos. Cell *90*, 707–716.
19. Thorpe, C.J., Schlesinger, A., Carter, J.C., and Bowerman, B. (1997). Wnt signaling polarizes an early *C. elegans* blastomere to distinguish endoderm from mesoderm. Cell *90*, 695–705.
20. Bei, Y., Hogan, J., Berkowitz, L.A., Soto, M., Rocheleau, C.E., Pang, K.M., Collins, J., and Mello, C.C. (2002). SRC-1 and Wnt signaling act together to specify endoderm and to control cleavage orientation in early *C. elegans* embryos. Dev. Cell *3*, 113–125.
21. Peters, J.M., McKay, R.M., McKay, J.P., and Graff, J.M. (1999). Casein kinase 1 transduces Wnt signals. Nature *401*, 345–350.
22. Walston, T., Tuskey, C., Edgar, L., Hawkins, N., Ellis, G., Bowerman, B., Wood, W., and Hardin, J. (2004). Multiple Wnt signaling pathways converge to orient the mitotic spindle in early *C. elegans* embryos. Dev. Cell *7*, 831–841.
23. Liu, J., Vasudevan, S., and Kipreos, E.T. (2004). CUL-2 and ZYG-11 promote meiotic anaphase II and the proper placement of the anterior-posterior axis in *C. elegans*. Development *131*, 3513–3525.
24. Sonneville, R., and Gonczy, P. (2004). Zyg-11 and Cul-2 regulate progression through meiosis II and polarity establishment in *C. elegans*. Development *131*, 3527–3543.
25. Yamanaka, A., Yada, M., Imaki, H., Koga, M., Ohshima, Y., and Nakayama, K. (2002). Multiple Skp1-related proteins in *Caenorhabditis elegans*: diverse patterns of interaction with cullins and F-box proteins. Curr. Biol. *12*, 267–275.
26. Nayak, S., Santiago, F.E., Jin, H., Lin, D., Schedl, T., and Kipreos, E.T. (2002). The *Caenorhabiditis elegans* Skp1-related gene family: diverse functions in cell proliferation, morphogenesis, and meiosis. Curr. Biol. *12*, 277–287.
27. Guo, S., and Kemphues, K.J. (1995). *par-1*, a gene required for establishing polarity in *C. elegans* embryos, encodes a putative Ser/Thr kinase that is asymmetrically distributed. Cell *81*, 611–620.
28. Himpel, S., Tegge, W., Frank, R., Leder, S., Joost, H.G., and Becker, W. (2000). Specificity determinants of substrate recognition by the protein kinase DYRK1A. J. Biol. Chem. *275*, 2431–2438.
29. Boxem, M., Srinivasan, D.G., and van den Heuvel, S. (1999). The *Caenorhabditis elegans* gene *ncc-1* encodes a cdc2-related kinase required for M phase in meiotic and mitotic cell divisions, but not for S phase. Development *126*, 2227–2239.
30. Polinko, E.S., and Strome, S. (2000). Depletion of Cks homolog in *C. elegans* embryos uncovers a post-metaphase role in both meiosis and mitosis. Curr. Biol. *10*, 1471–1474.
31. Jeffrey, P.D., Russo, A.A., Polyak, K., Gibbs, E., Hurwitz, J., Massague, J., and Pavletich, N.P. (1995). Mechanism of CDK activation revealed by the structure of a cyclinA-CDK2 complex. Nature *376*, 313–320.
32. Bourne, Y., Watson, M.H., Hickey, M.J., Holmes, W., Rocque, W., Reed, S.I., and Tainer, J.A. (1996). Crystal structure and mutational analysis of the human CDK2 kinase with cell cycle-regulatory protein CksHs1. Cell *84*, 863–874.
33. Nieduszynski, C.A., Murray, J., and Carrington, M. (2002). Whole-genome analysis of animal A- and B-type cyclins. Genome Biol. *3*, 0070.1–0070.8.
34. van den Heuvel, S. (2005). The *C. elegans* cell cycle: overview of molecules and mechanisms. Methods Mol. Biol. *296*, 51–67.
35. Lai, W.S., Carballo, E., Strum, J.R., Kennington, E.A., Phillips, R.S., and Blackshea, P.J. (1999). Evidence that tristetraprolin binds to AU-rich elements and promotes the deadenylation and destabilization of tumor necrosis factor alpha mRNA. Mol. Cell. Biol. *19*, 4311–4323.
36. Schneider, S.Q., and Bowerman, B. (2003). Cell polarity and the cytoskeleton in the *Caenorhabditis elegans* zygote. Annu. Rev. Genet. *37*, 221–249.
37. Stitzel, M.L., Pellettieri, J., and Seydoux, G. (2005). The *C. elegans* DYRK kinase MBK-2 marks oocyte proteins for degradation in response to meiotic maturation. Curr. Biol. *16*, this issue, 56–62. Published online December 8, 2005. 10.1016/j.cub.2005.11.063.
38. Nishi, Y., and Lin, R. (2005). DYRK2 and GSK-3 phosphorylate and promote the timely degradation of OMA-1, a key regulator of the oocyte-to-embryo transition in *C. elegans*. Dev. Biol. *288*, 139–149. Published online November 10, 2005. 10.1016/j.ydbio.2005.09.053.
39. Tio, M., Udolph, G., Yang, X., and Chia, W. (2001). *cdc2* links the *Drosophila* cell cycle and asymmetric division machineries. Nature *409*, 1063–1067.
40. Yu, V.P., Baskerville, C., Grunenfelder, B., and Reed, S.I. (2005). A kinase-independent function of Cks1 and Cdk1 in regulation of transcription. Mol. Cell *17*, 145–151.

Note Added in Proof

In the version of this paper originally published online on December 8, 2005, Figure 6B did not indicate the gradient distribution of MEX-5 in the 1-cell stage. The figure has been corrected here.
Reference [38], which had previously been in press, has been updated to include full publication information for the article.